ANTIOXIDANTS & REDOX SIGNALING
Volume 8, Numbers 9 & 10, 2006

Original Research Communication

Copper Activates the NF-κB Pathway *In Vivo*

TIZIANA PERSICHINI,[1] ZULEMA PERCARIO,[1] EMANUELA MAZZON,[2]
MARCO COLASANTI,[1] SALVATORE CUZZOCREA,[2] and GIOVANNI MUSCI[3]

ABSTRACT

Previous results indicated that intravenous injection of copper in the form of a copper–histidine complex in rats triggers the transcriptional induction of the inducible form of nitric oxide synthase (NOS-II). Here, the authors demonstrate that copper activates the transcription factor NF-κB in the liver and lung tissues of rats, and that this effect is mediated by oxidative stress, since all copper-induced changes, which include histological alterations, formation of nitrotyrosines, vascular pressure drop, production of tumor necrosis factor-α (TNF-α), induction of NOS-II and nitrites, are readily prevented by pretreatment of the animals with the antioxidant tempol. By using electrophoretic mobility shift assays, the p50/p65 dimer and higher molecular weight aggregates have been found to be involved in the copper-induced NF-κB activation. COX-2, a NF-κB-dependent gene involved in the inflammatory response, was also transcriptionally induced by copper, this effect being reduced in the presence of tempol. These results suggest that a physiopathological status, characterized by hypercupremic situations, may lead to the onset of inflammation through production of ROS and activation of NF-κB. *Antioxid. Redox Signal.* 8, 1897–1904.

INTRODUCTION

The members of NF-κB transcription factors of the Rel family proteins are p65 (RelA), p50, p52, c-Rel, and RelB. In unstimulated cells, NF-κB, frequently under the form of a p50/p65 dimer, resides in a latent form in the cytoplasm bound to the inhibitory subunit IκB (1, 2). Upon cell stimulation, IκB is removed and the liberated NF-κB translocates into the nucleus and activates target genes by binding to regulatory elements in enhancers and promoters. The removal of IκB is controlled by protein phosphorylation and subsequent rapid degradation by the 20 S or 26 S proteasome (19, 31). Specific peptide inhibitors of the proteasome that stabilize the phosphoform of IκB are potent inhibitors of NF-κB activation.

A number of distinct stimuli, including infections, inflammatory cytokines, radiations, and oxidants are known to post-transcriptionally activate NF-κB (3, 17, 28). Many of these stimuli cause oxidative stress in cells, with overproduction of reactive oxygen species (ROS) such as superoxide, hydrogen peroxide, and hydroxyl radicals (24, 25). NF-κB activation is thought to be a direct consequence of oxidative stress on the basis of several lines of evidence. These include the notion that NF-κB activation can be suppressed by structurally unrelated antioxidants such as dithiocarbamates (26), NAC (27), and vitamin E derivatives (29); the ability of hydrogen peroxide to act as an activator of NF-κB in some cell lines (18, 27); and the observation that stable overexpression of catalase impairs NF-κB activation, whereas overexpression of Cu/Zn superoxide dismutase superinduces NF-κB activation in response to TNF-α (23). Antioxidants also prevent the decay of IκB; however, they inhibit the phosphorylation step rather than the proteasome. Hence, antioxidants may act upstream of the kinase/phosphatase system, suggesting that the IκB phosphorylation is redox-controlled.

There is, however, a consistent body of literature claiming that ROS are not activators, but rather inhibitors for NF-κB (4, 15). A central role for oxidative stress in NF-κB activation

[1]Dipartimento di Biologia, Università Roma Tre, Rome, Italy.
[2]Dipartimento Clinico-sperimentale di Medicina e Farmacologia, Università di Messina, Messina, Italy.
[3]Dipartimento di Scienze e Tecnologie Agro-alimentari, Ambientali e Microbiologiche, Università del Molise, Campobasso, Italy.

seems to be ruled out by evidence such as the cell specificity of hydrogen peroxide-induced activation of NF-κB, and the involvement of redox-independent targets in the inhibitory effect of antioxidants (4). In this respect, recent findings demonstrated that NAC and pyrrolidine dithiocarbamate, compounds widely recognized as potential antioxidants, can inhibit TNF-α-induced NF-κB activation independently of antioxidative function, either by lowering the affinity of receptor to TNF-α, or by inhibiting NF-κB activation in cell-free systems, where extracellular stimuli-regulated ROS production does not occur (12). Thus, according to this view, in most cases, the role of oxidative stress in NF-κB activation is at best facilitatory rather than causal, if a role exists at all.

Copper is an integral part of many important enzymes involved in a number of vital biological processes. Although this metallic ion is usually bound to proteins, it may be released and become free to catalyze the formation of highly reactive hydroxyl radicals. For this reason, copper has been largely involved in the onset of oxidative stress (32), at least in *in vitro* and cell culture studies. Oxidative damage induced by copper may be involved in a number of pathologies, with particular regard to neurodegenerative conditions such as Alzheimer's disease, familial amyotrophic lateral sclerosis, and prion diseases. However, the finding that the upper limit of "free pools" of copper is far less than a single atom per cell casts serious doubt on the *in vivo* role of copper in Fenton-like generation of free radicals (21).

We have recently demonstrated that serum copper elevation induced by i.v. injection of the metal ends up in massive activation of NOS-II in rats. To better understand the mechanisms leading to *in vivo* NOS-II activation by copper, we have analyzed the role of oxidative stress, on one hand, and the possible involvement of NF-κB, on the other.

MATERIALS AND METHODS

Chemicals

All reagents and compounds used were obtained from Sigma Chemical Company (Milan, Italy), unless otherwise stated. The Cu–His complex was prepared by adding 1 mol of $CuCl_2$ to 3 mols of L-histidine in water (8).

Animals and experimental groups

Male Sprague–Dawley rats (200–250 g; Charles River, Milan, Italy) were housed in a controlled environment and provided with standard rodent chow and water. Animal care was in compliance with Italian regulations on protection of animals used for experimental and other scientific purposes (D.M. 116192), as well as with the EEC regulations (O.J. of E.C. L 358/1 12/18/1986). Rats were anesthetized with urethane (1.3 g/kg. i.p.). The trachea was cannulated to facilitate respiration, and body temperature was maintained at 37°C by means of a heating pad. Following anesthesia, catheters were placed in the carotid artery and jugular vein, as described previously (6). Blood pressure was monitored continuously by a Maclab A/D converter (Ugo Basile, Varese, Italy), and stored and displayed on Macintosh personal computer. The left femoral vein was cannulated for administration of drugs. After recording baseline hemodynamic parameters, animals were divided into four groups according to treatments: (a) Cu–His group (n = 10): Cu–His (1 m*M*) given as a slow i.v. bolus injection (0.3 ml volume) over 2 min; (b) Cu–His + tempol group (n = 10): tempol (100 mg/kg i.v. bolus injection) was administered 15 min prior to Cu–His (1 m*M*); (c) sham group (n = 10) in which surgical procedures identical to the Cu–His group were performed, except that saline was administered instead of Cu–His; and (d) sham-tempol group (n = 10), in which surgical procedures identical to the Cu–His + tempol group were performed, except that tempol alone was administered.

Light microscopy and immunohistochemistry

Lung and liver samples were taken 4 h after treatment. The tissue slices were fixed in Dietric solution [14.25% (vol/vol) ethanol, 1.85% (wt/vol) formaldehyde, 1% (vol/vol) acetic acid] for 1 week at room temperature, dehydrated by graded ethanol, and embedded in Paraplast (Sherwood Medical, Mahwah, New Jersey). Sections (thickness 7 μm) were deparaffinized with xylene, stained with hematoxylin and eosin (lung) or by trichrome stain (liver), and observed in Dialux 22 Leitz microscope..

NOS-II was determined in different tissues by immunohistochemistry as previously described (8). Briefly, tissues were fixed in 10% (wt/vol) PBS-buffered formalin and 8 μm sections were prepared from paraffin embedded tissues. After deparaffinization, endogenous peroxidase was quenched with 0.3% (vol/vol) hydrogen peroxide in 60% (vol/vol) methanol for 30 min. The sections were permeabilized with 0.1% (vol/vol) Triton X-100 in PBS for 20 min. Nonspecific adsorption was minimized by incubating the section in 2% (vol/vol) normal goat serum in PBS for 20 min. Endogenous biotin or avidin binding sites were blocked by sequential incubation for 15 min with avidin and biotin (DBA, Milan, Italy). The sections were then incubated overnight with 1:1,000 dilution of primary anti-NOS-II antibody (DBA), or with control solutions. Controls included buffer alone or nonspecific purified rabbit IgG. Specific labeling was detected with a biotin-conjugated specific secondary anti-IgG and avidin–biotin peroxidase complex (DBA). To verify the binding specificity for NOS-II, some sections were also incubated with primary antibody only (no secondary antibody) or with secondary antibody only (no primary antibody). In these situations, no positive staining was found in the sections, indicating that the immunoreactions were positive in all the experiments carried out.

Immunocytochemistry photographs (n = 5) were assessed by densitometry by using an Imaging Densitometer (AxioVision, Zeiss, Milan, Italy) and the related software from the manufacturer.

Measurement of NO_x and TNF-α

Nitrite/nitrate (NO_x), the breakdown products of NO, and TNF-α levels were measured in plasma samples from the different groups 4 h after the specific treatment. To measure NO_x, nitrate in the plasma was first reduced to nitrite by incubation with nitrate reductase (670 mU/ml) and NADPH (160 μ*M*) at room temperature for 3 h. Nitrite concentration in the

samples was then measured by the Griess reaction, by adding 100 µl of Griess reagent (0.1% NEDA in H_2O and 1% sulfanilamide in 5% concentrated H_3PO_4; vol. 1:1) to 100 µl samples. The optical density at 550 nm (OD_{550}) was measured using a Spectramax 250 microplate reader (Molecular Devices, Sunnyvale, CA). Nitrite concentrations were calculated by comparison with OD_{550} of standard solutions of sodium nitrite prepared in saline solution.

TNF-α was evaluated by using a colorimetric, commercial kit (Calbiochem–Novabiochem, La Jolla, CA). The enzyme linked immunosorbent assay has a lower detection limit of 5 pg/ml.

Quantification of NF-κB activation by ELISA

NF-κB activation was quantified using a TransAM NF-κB kit (Active Motif, Rixensart, Belgium). Briefly, nuclear extracts were prepared from liver or lung tissues after homogenization with Dounce in buffer A (10 m*M* Hepes pH 7.9, 10 m*M* KCl, 3 m*M* $MgCl_2$, 0.1 m*M* EDTA, 0.1 m*M* EGTA, 0.5 m*M* DTT, 1 m*M* PMSF, 10 µg/ml aprotinin, and 10 µg/ml leupeptin). A second step was carried out in buffer A with 0.5% Igepal to separate nuclei from cytosol. After centrifugation at 200 *g* for 10 min at 4°C, pellets containing nuclear fractions were resuspended in buffer C (20 m*M* Hepes pH 7.9, 400 m*M* NaCl, 1 m*M* EDTA, 1 m*M* EGTA, 0.5 m*M* DTT, 1 m*M* PMSF, 10 µg/ml aprotinin, and 10 µg/ml leupeptin) and incubated on ice for 15 min. A final centrifugation at 12,000 *g* was carried out, and the supernatants were collected and quickly frozen in liquid nitrogen. Total protein content of extracts was determined according to Bradford (5). Ten µg/well of nuclear extracts were incubated in a 96-well plate on which a double-stranded oligonucleotide containing the NF-κB consensus site (5′-GGGACTTTCC-3′) had been immobilized. The primary antibody used to detect NF-κB recognized an epitope on p65 subunit that is accessible only when NF-κB is activated and bound to its target DNA. After incubation with a horseradish peroxidase-conjugated secondary antibody and the developing solution, absorbance was read at 450 nm, with a reference wavelength of 655 nm.

NF-κB dimer characterization by DNA Electrophoresis Mobility Shift Assay (EMSA)

Nuclear extracts from lung or liver tissues were prepared as described above. Three picomoles of the double-stranded oligonucleotide containing the NF-κB binding site of the NOS-II promoter (5′-AGTTGAGGGGACTTTCCCAGGC-3′) were end-labeled with [γ-^{32}P]ATP (74 MBq/ml, 220 TBq/mmol; Amersham Biosciences Europe GmbH) by T4 polynucleotide kinase (New England Biolabs, Beverly, MA). Extracts (8 µg) were incubated in the presence of the labeled oligonucleotide probe (40,000 cpm) at 4°C for 30 min and at room temperature for 40 min in 20 µl of binding buffer (20 m*M* Tris, pH 7.5, 75 m*M* KCl, 13% glycerol, 1 m*M* DTT, 1 µg of BSA, and 2 µg of poly(dI)/poly(dC)). Cold competitor was added in a 100-fold molar excess of the radiolabeled probe. Supershift was performed by using 1 µg of the specific antibodies recognizing different NF-κB subunits (anti-p50, anti-p65, anti-RelB,or anti-c-rel polyclonal antibodies; Santa Cruz Biotechnology, Santa Cruz, CA). DNA–protein complexes were resolved on 5% polyacrylamide gels in 25 m*M* Tris-borate buffer, pH 8.2, 0.5 m*M* EDTA, and were visualized by autoradiography.

mRNA expression by reverse transcriptase–polymerase chain reaction (RT–PCR)

RT–PCR was carried out on total cellular RNA purified from the homogenized tissues by using the RNA Fast Isolation Reagent (Molecular System, San Diego, CA) and reverse transcribed into cDNA using MMLV reverse transcriptase and oligo dT(12–18) as primers. cDNA was amplified for the COX-2 gene (297 bp) using specific primers (Ambion, Inc. Woodward, Austin, TX). The mRNA for the constitutive GAPDH enzyme was examined as the reference cellular transcript, and it was found to be present at comparable levels in all tissue lysates. Estimates of the relative mRNA amounts were obtained by dividing the area of the COX-2 band by the area of the GAPDH band (Bio-Rad Multi-Analyst™/PC Version 1.1). Molecular weight was the 100-bp DNA ladder (Life Technologies, Inc.).

Data analysis

All values are expressed as mean ± standard error of the mean (SEM) of *n* observations. For the *in vivo* studies, *n* represents the number of animals studied. In the experiments involving histology or immunohistochemistry, the figures shown are representative of at least three experiments performed on different experimental days. The results were analyzed by one-way ANOVA, followed by a Bonferroni's *posthoc* test for multiple comparisons, or by two-way analysis of variance with the *F* statistic to test for independent effects of treatments and time.

RESULTS

Effect of tempol on copper-challenged rats

We have previously reported that rats treated with copper (administered as a Cu–His complex) show massive induction of NOS-II and formation of nitrotyrosines (an indicator of peroxynitrite production) in liver and lung tissues, comparable to that attained after LPS treatment (8). To ascertain the involvement of oxidative stress in the observed NOS-II induction, rats were treated with Cu–His after preinjection of a bolus of 100 mg/kg tempol, and sections of lung and liver were analyzed 4 h after challenge. The results are reported in Fig. 1. As can be clearly seen, the effect of copper was efficiently counteracted by treatment with the antioxidant, which significantly prevented the NOS-II (panels A, C) and nitrotyrosines (panels B, C) positive staining induced by the metal. No staining for NOS-II or nitrotyrosines was observed in lung and liver sections obtained from sham-operated rats. A densitometric analysis performed on several standard fields confirmed that the effect of tempol was statistically significant (Fig. 1, panel C).

Copper has also been reported to cause severe NO-dependent tissue injury in lung and liver (8). Therefore, histological

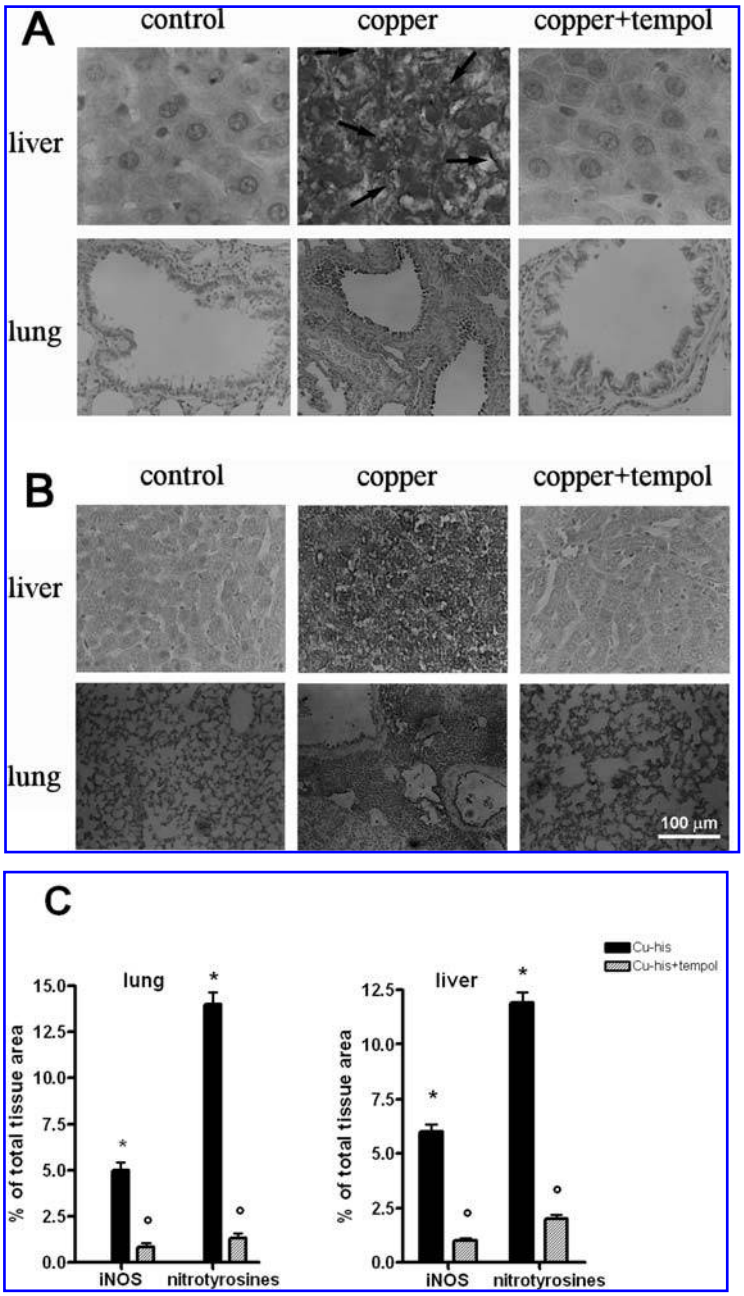

FIG. 1. Immunohistochemical localization of NOS-II (*panel A*) and nitrotyrosines (*panel B*) in the liver and in the lung. Four hours after Cu–His, positive NOS-II and nitrotyrosine staining was found in both tissues. There was essentially no detectable immunostaining in the liver or lung of rats treated with tempol before injection of Cu–His. Original magnification: 128.5X. Figure is representative of at least three experiments performed on different experimental days. *Arrows* indicate positive hepatocytes. *Panel C* is the densitometric analysis of several sample fields ($n = 5$). Values from the sham group were undetectable. Statistics: (*), $p < 0.001$ Cu–His vs. sham; (°), $p < 0.05$ Cu–His + tempol vs. Cu–His group.

examination was carried out on sections of lung and liver from rats challenged with copper for 4 h after injection of tempol. As expected, the pathological changes induced by copper were efficiently prevented by tempol (Fig. 2). In particular, necrosis of hepatocytes in the liver, and extravasation of red cells and inflammatory cell accumulation in the lung were significantly reduced in tempol-treated rats.

To further confirm that tempol was efficient in reducing copper-induced physiological alterations of nitric oxide metabolism, we have examined three more parameters previously found to be affected: vascular pressure, accumulation of nitrite/nitrate in the plasma, and presence of TNF-α in the blood. When compared to sham, treatment with Cu–His showed a significant decrease of the mean arterial blood pressure (F, 241.4 [$p < 0.0001$]). This effect was reverted by treatment with tempol (F, 55.31 [$p < 0.001$]), differences being statistically significant already after 4 h of treatment (Fig. 3A). Likewise, levels of nitrite/nitrate (Fig. 3B), and of TNF-α (Fig. 3C), both indicative of NO production, were markedly increased ($p < 0.001$) in the plasma from rats challenged with copper, but significantly ($p < 0.01$) reduced toward basal levels in animals preinjected with tempol.

NF-κB activation and dimer characterization

To assess whether NF-κB was activated in the liver and lung of copper-challenged rats, the extent of NF-κB activation was evaluated at different times (15, 30, 60, and 180 min)

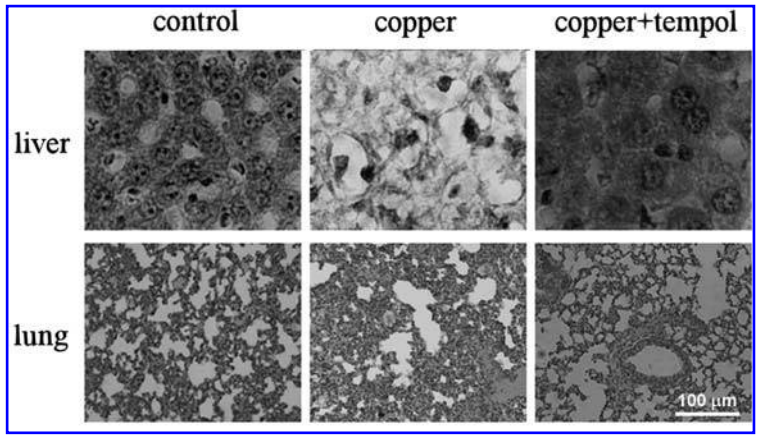

FIG. 2. Morphology of liver and lung. Representative liver sections from Cu–His-treated rats demonstrate hepatic damage, characterized by necrosis of hepatocytes. Representative lung sections from Cu–His-treated rats demonstrate inflammatory cells infiltration. Liver and lung sections from rats pretreated with tempol demonstrate reduced liver injury and reduced inflammatory cells infiltration, respectively. Original magnification: 125X. Figure is representative of at least three experiments performed on different experimental days.

as the increase of binding activity to a specific target sequence in an ELISA assay. As shown in Fig. 4A, treatment with copper induced an early activation of NF-κB, which peaked after a 60-min stimulation (Fig. 4A). Pretreatment of rats with tempol was able to inhibit copper-elicited NF-κB activation (Fig. 4A), again suggesting that oxidative stress is involved in this mechanism. Similar results were observed in the lung of copper-challenged rats (Fig. 4B).

The NF-κB subunits involved in the copper-induced NF-κB activation were analyzed by EMSA (Fig. 5). A lysate from the liver of animals treated with copper for 60 min (lane 4) showed the presence of two shifted components (*arrows*). Consistent with the ELISA data above, NF-κB activation was efficiently prevented by tempol (lane 3). When the liver lysate was incubated with antibodies specifically recognizing the p50, the p65, RelB, or c-rel NF-κB subunits, or, as a control, with a cold competitor, both shifted bands turned out to be efficiently super-shifted by the anti-p65 and anti-p50 antibodies (lanes 5 and 6, respectively), but not by anti-RelB or anti-c-rel (lanes 7 and 8), clearly indicating the presence of the p50/p65 heterodimer in both components. Similar results were obtained with the lung (data not shown).

COX-2 mRNA expression by RT–PCR

To prove that other NF-κB-dependent genes besides NOS-II and TNF-α were transcriptionally switched on in the liver of copper-challenged rats, COX-2 mRNA expression levels were analyzed using RT–PCR. As shown in Fig. 6, the expected 297 bp fragment was readily amplified in animals treated with copper for 3 h. As expected, the copper-induced expression of COX-2 mRNA was inhibited by preadministration of tempol.

DISCUSSION

In this manuscript, we present the first *in vivo* evidence that copper can activate NF-κB and transcriptionally induce NF-κB-dependent genes such as NOS-II, TNF-α, and COX-2 through production of reactive oxygen species. As already pointed out in a previous paper (8), the induction of NOS-II has dramatic consequences for the animal, including a significant drop of the vascular pressure (which ultimately leads to death) and the significant impairment of histological parameters of liver and lung. To test directly whether oxidative stress is involved in these effects, we used tempol, which permeates biological membranes and scavenges superoxide anions (7). All these changes are readily prevented when the animal is pretreated with the antioxidant tempol before copper challenge. Moreover, the massive formation of nitrotyrosines in all examined tissues following copper injection, indicative that synthesis of peroxynitrite occurs, is also strongly prevented in the presence of tempol.

Conflicting results have been presented in the last two decades on the effect of oxidative stress on the transcription factor NF-κB (4, 12, 15, 18, 23, 26, 27, 29). Moreover, although copper is naturally recognized as an inducer of oxidative stress (32), little is known on its effects *in vivo*, most studies dealing with cellular models. Intracellular concentrations of free copper may be well below the threshold for efficient Fenton reaction to occur (21), which makes the role of copper *in vivo* even more uncertain with respect to ROS production.

Our data are straightforward in demonstrating that elevation of serum copper triggers a massive oxidative stress, as shown by the highly significant effect of tempol on all changes induced by the metal. The effect of tempol is consistent with previous data on copper-induced nitrotyrosines production in different tissues (8), and indeed we show here that nitrotyrosines do not form when the antioxidant is administered along with copper. The oxidative stress triggered by copper results in activation of NF-κB under the classical form of a p50/p65 heterodimer, as shown by EMSA, supporting the idea that the activation of the NF-κB transcription complex is part of the inflammatory response to copper. As a matter of fact, copper-evoked activation of NF-κB leads in turn to transcriptional switch on of a number of inflammatory genes, including NOS-II, TNF-α, and COX-2. It should be noted that our data suggest that a higher molecular weight complex is involved besides the p50/p65 heterodimer. As a matter of fact, the super-shift experiments show that the copper-induced shifted bands both contain p50 and p65, since they are sensitive to both anti-p65 and anti-p50 antibodies. It can be therefore safely speculated that the higher mobility band is due to the p50/p65 heterodimer, while the lower mobility

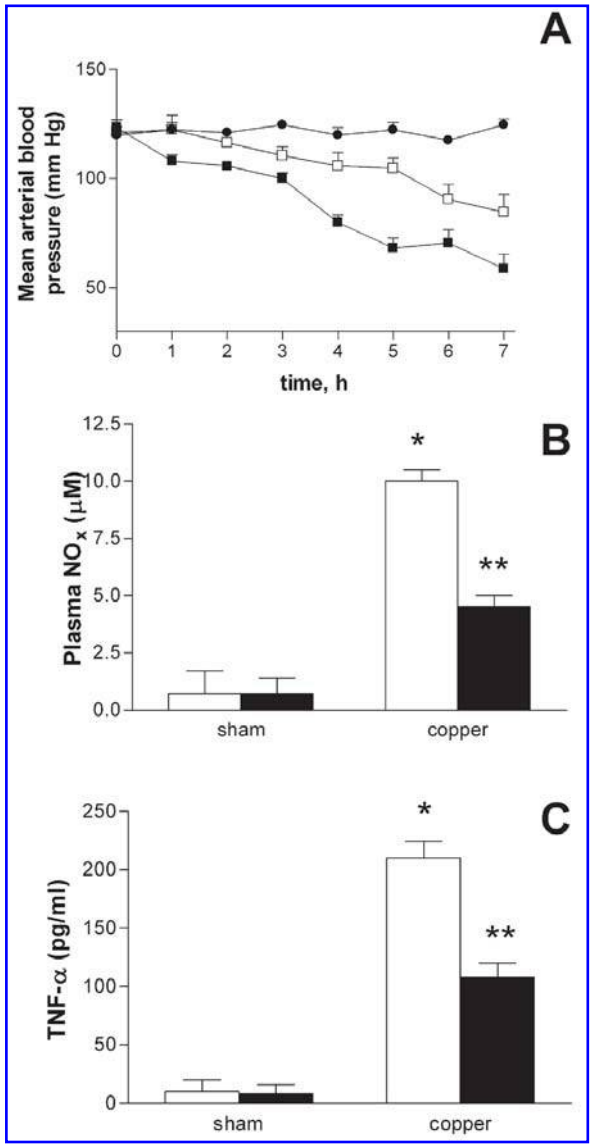

FIG. 3. Vascular parameters of copper-treated rats. Mean arterial pressure (*panel A*), plasma levels of NOx (*panel B*), and TNF-α (*panel C*) in rats treated with copper and/or tempol. Symbols used for different treatments in *panel A*: •, sham group; ■, Cu–His; □, tempol + Cu–His. *Panels B* and *C*: clear bars: without tempol pretreatment; filled bars, with tempol pretreatment. Statistics: *panel A*, Cu–His vs. sham F, 241.4 ($p < 0.0001$); Cu–His vs Cu–His + tempol F, 55.31 ($p < 0.001$). *Panel B* and *C*, (*) $p < 0.001$ Cu–His vs. sham; (**) $p < 0.001$ Cu–His + tempol vs. Cu–His.

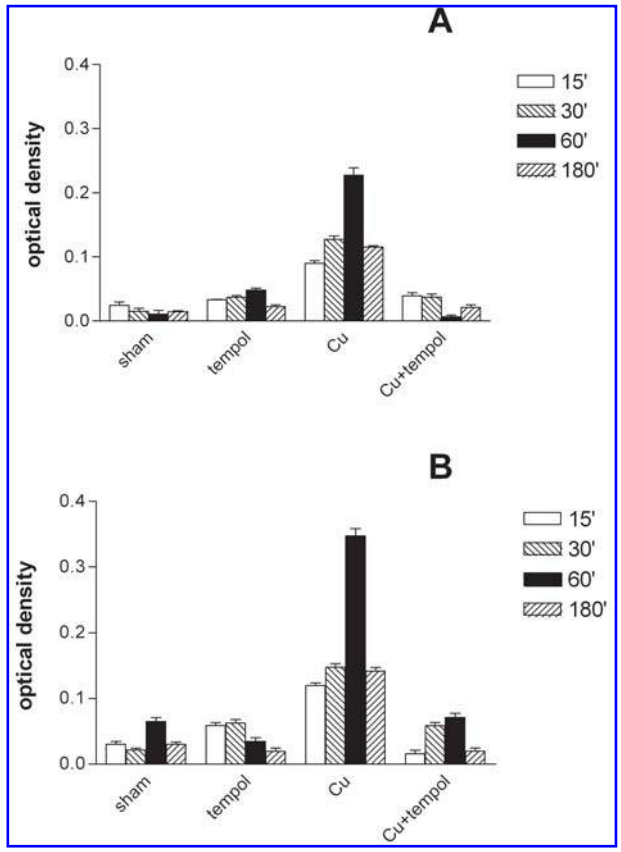

FIG. 4. Quantification of NF-κB activation by ELISA. Effect of tempol on copper-induced NF-κB activation in the liver (**A**) and lung (**B**) tissues. The extent of NF-κB activation was evaluated at different times (15, 30, 60, and 180 min) as the increase of binding activity to a specific consensus sequence in an ELISA assay (for further details see "Materials and Methods" section). *Bars* represent the absorbance at 450 nm with a reference wavelength of 655 nm. Statistics: $p < 0.001$ Cu–His vs. sham at all times tested; $p < 0.001$ Cu–His + tempol vs. Cu–His at all times tested.

band arises from p50/p65 complexing of additional transcription factors. In this respect, a number of coactivators (*e.g.*, p300, CBP, Sp1, CPAP, SIMPL, and RHA) have been described to interact with the p65 subunit (13, 14, 20, 30, 34). Further studies are in progress to better specify the component of the transactivation complex that appears to mediate the transcriptional activity of NF-κB induced by copper.

We are reminded that, although cells readily uptake copper through several molecular mechanisms (10, 11, 16), copper apparently does not enter tissue cells under our conditions, as shown by the unchanged metal content of lung or liver after copper–histidine injection (8). Although cellular enrichment in copper content might be very difficult to catch because of its transient kinetics, this suggests that the oxidative stress is induced in the plasma, and is then transduced within the cells, leading to the inflammatory cascade. However, a ROS generation at intracellular level can not be excluded. Indeed, total copper content into a tissue does not necessarily reflect the intracellular copper level, because an acute impairment of copper traffic can lead to redistribution of the metal into the various cellular compartments and consequent modification of its biological activity.

While little is known on the chronic effects of elevated serum copper levels, apart from isolated evidence on the association with atherosclerosis (9), myocardial infarction (22), and stroke and pregnancy-induced hypertension (33), even less data are available on the consequences of acute serum copper elevation. We are the first to show that this status,

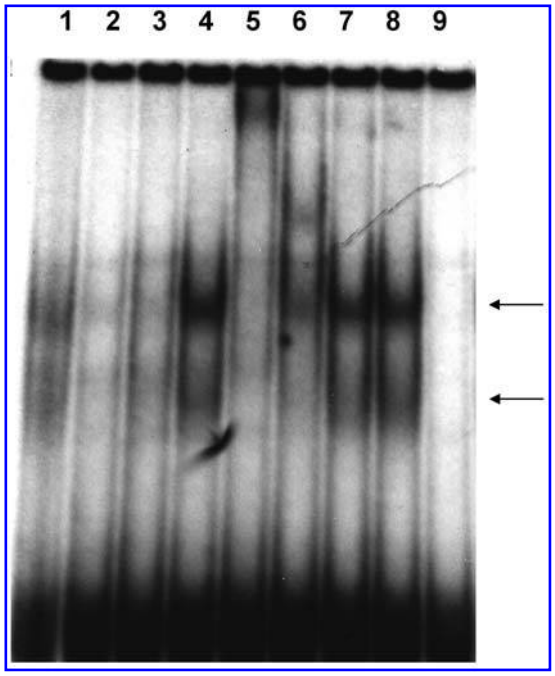

FIG. 5. DNA Electrophoretic Mobility Shift Assay (EMSA). Labeled oligonucleotide probe (40,000 cpm) containing NOS-II promoter NF-κB binding site was incubated with 8 μg nuclear extracts of liver tissue derived from sham-treated rats in the absence (*lane 1*) or presence (*lane 2*) of tempol, or from rats challenged with Cu–His for 1 h in the presence (*lane 3*) or absence (*lanes 4–8*) of tempol. To characterize the NF-κB protein involved specific antibodies were used: anti-p65 (*lane 5*), anti-p50 (*lane 6*), anti-cRel (*lane 7*), and anti-Rel B (*lane 8*). As a specific control of DNA-NF-κB protein binding, cold competitor was added in 100-fold molar excess of radiolabeled probe (*lane 9*).

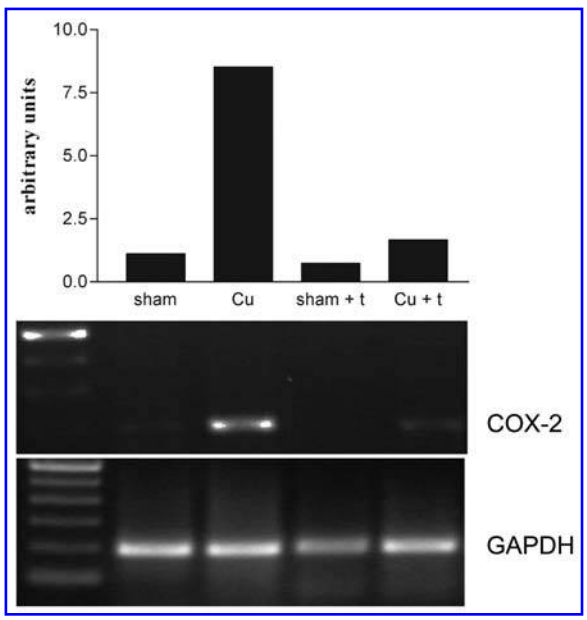

FIG. 6. COX-2 mRNA expression. Effect of tempol (t) on copper-induced COX-2 mRNA expression in the liver.

which can be pathologically achieved upon heavy metal intoxication, or physiologically attained in naturally occurring hypercupremic situations such as pregnancy, leads to the onset of inflammation through production of ROS and activation of NF-κB.

ACKNOWLEDGMENTS

This work was supported by PRIN 2000 and PRIN 2002 from the Italian Minister of Instruction, University and Research, and by grants from EU Commission (Project ZINCAGE, no. FOOD-CT-2003–506850).

ABBREVIATIONS

CBP, CREB binding protein; CPAP, centrosomal P4.1-associated protein; EDTA, ethylenediaminetetraacetic acid; EGTA, ethylene glycol-bis(β-aminoethyl ether) *N*, *N*, *N*^{9}, *N*^{9}-tetraacetic acid; ELISA, enzyme-linked immune-absorbent assay; EMSA, electrophoretic mobility shift assay; GAPDH, glyceraldeyde-3-phosphate dehydrogenase; HEPES, *N*-2-hydroxyethylpiperazine *N*-2-ethanesulfonic acid; LPS, *E. coli* lipopolysaccharide; NAC, *N*-acetyl-L-cysteine; NEDA, *N*-(1-naphthyl) ethylenediamine dihydrochloride; NO, nitric oxide, NOS-II, inducible nitric oxide synthase; PBS, phosphate-buffered saline; PMSF, phenyl-methyl sulfonyl fluoride; RHA, RNA helicase A; ROS, reactive oxygen species; RT–PCR, reverse transcriptase–polymerase chain reaction; SIMPL, signaling molecule that interacts with mouse pelle-like kinase; TNFα, tumor necrosis factor α.

REFERENCES

1. Baeuerle PA and Baltimore D. Activation of DNA-binding activity in an apparently cytoplasmic precursor of the NF-kappa B transcription factor. *Cell* 53: 211–217, 1988.
2. Baeuerle PA and Baltimore D. I kappa B: a specific inhibitor of the NF-kappa B transcription factor. *Science* 242: 540–546, 1988.
3. Baeuerle PA and Henkel T. Function and activation of NF-kappa B in the immune system. *Annu Rev Immunol* 12: 141–179, 1994.
4. Bowie A and O'Neill LA. Oxidative stress and nuclear factor-kappaB activation: a reassessment of the evidence in the light of recent discoveries. *Biochem Pharmacol* 59: 13–23, 2000.
5. Bradford MM. A rapid and sensitive method for the quantitation of microgram quantities of protein utilizing the principle of protein-dye binding. *Anal Biochem* 72: 248–254, 1976.
6. Caputi AP, Rossi F, Carney K, and Brezenoff HE. Modulatory effect of brain acetylcholine on reflex-induced bradycardia and tachycardia in conscious rats. *J Pharmacol Exp Ther* 215: 309–316, 1980.
7. Cuzzocrea S, McDonald MC, Filipe HM, Costantino G, Mazzon E, Santagati S, Caputi AP, and Thiemermann C.

Effects of tempol, a membrane-permeable radical scavenger, in a rodent model of carrageenan-induced pleurisy. *Eur J Pharmacol* 390: 209–222, 2000.
8. Cuzzocrea S, Persichini T, Dugo L, Colasanti M, and Musci G. Copper induces type II nitric oxide synthase *in vivo*. *Free Radic Biol Med* 34: 1253–1262, 2003.
9. Ferns GA, Lamb DJ, and Taylor A. The possible role of copper ions in atherogenesis: the Blue Janus. *Atherosclerosis* 133: 139–152, 1997.
10. Harris ED. Cellular copper transport and metabolism. *Annu Rev Nutr* 20: 291–310, 2000.
11. Harris ED. Copper homeostasis: the role of cellular transporters. *Nutr Rev* 59: 281–285, 2001.
12. Hayakawa M, Miyashita H, Sakamoto I, Kitagawa M, Tanaka H, Yasuda H, Karin M, and Kikugawa K. Evidence that reactive oxygen species do not mediate NF-kappaB activation. *EMBO J* 22: 3356–3366, 2003.
13. Koyanagi M, Hijikata M, Watashi K, Masui O, and Shimotohno K. Centrosomal P4.1-associated protein is a new member of transcriptional coactivators for nuclear factor-kappaB. *J Biol Chem* 280: 12430–12437, 2005.
14. Kwon HJ, Breese EH, Vig-Varga E, Luo Y, Lee Y, Goebl MG, and Harrington MA. Tumor necrosis factor alpha induction of NF-kappaB requires the novel coactivator SIMPL. *Mol Cell Biol* 24: 9317–9326, 2004.
15. Li N and Karin M. Is NF-kappaB the sensor of oxidative stress? *FASEB J* 13: 1137–1143, 1999.
16. Linder MC, Lomeli NA, Donley S, Mehrbod F, Cerveza P, Cotton S, and Wotten L. Copper transport in mammals. *Adv Exp Med Biol* 448: 1–16, 1999.
17. Liou HC and Baltimore D. Regulation of the NF-kappa B/rel transcription factor and I kappa B inhibitor system. *Curr Opin Cell Biol* 5: 477–487, 1993.
18. Meyer M, Schreck R, and Baeuerle PA. H2O2 and antioxidants have opposite effects on activation of NF-kappa B and AP-1 in intact cells: AP-1 as secondary antioxidant-responsive factor. *EMBO J* 12: 2005–2015, 1993.
19. Palombella VJ, Rando OJ, Goldberg AL, and Maniatis T. The ubiquitin-proteasome pathway is required for processing the NF-kappa B1 precursor protein and the activation of NF-kappa B. *Cell* 78: 773–785, 1994.
20. Perkins ND, Agranoff AB, Pascal E, and Nabel GJ. An interaction between the DNA-binding domains of RelA(p65) and Sp1 mediates human immunodeficiency virus gene activation. *Mol Cell Biol* 14: 6570–6583, 1994.
21. Rae TD, Schmidt PJ, Pufahl RA, Culotta VC, and O'Halloran TV. Undetectable intracellular free copper: the requirement of a copper chaperone for superoxide dismutase. *Science* 284: 805–808, 1999.
22. Reunanen A, Knekt P, Marniemi J, Maki J, Maatela J, and Aromaa A. Serum calcium, magnesium, copper and zinc and risk of cardiovascular death. *Eur J Clin Nutr* 50: 431–437, 1996.
23. Schmidt KN, Traenckner EB, Meier B, and Baeuerle PA. Induction of oxidative stress by okadaic acid is required for activation of transcription factor NF-kappa B. *J Biol Chem* 270: 27136–27142, 1995.
24. Schreck R, Albermann K, and Baeuerle PA. Nuclear factor kappa B: an oxidative stress-responsive transcription factor of eukaryotic cells (a review). *Free Radic Res Commun* 17: 221–237, 1992.
25. Schreck R and Baeuerle PA. A role for oxygen radicals as second messengers. *Trends Cell Biol* 1: 39–42, 1991.
26. Schreck R, Meier B, Mannel DN, Droge W, and Baeuerle PA. Dithiocarbamates as potent inhibitors of nuclear factor kappa B activation in intact cells. *J Exp Med* 175: 1181–1194, 1992.
27. Schreck R, Rieber P, and Baeuerle PA. Reactive oxygen intermediates as apparently widely used messengers in the activation of the NF-kappa B transcription factor and HIV-1. *EMBO J* 10: 2247–2258, 1991.
28. Siebenlist U, Franzoso G, and Brown K. Structure, regulation and function of NF-kappa B. *Annu Rev Cell Biol* 10: 405–455, 1994.
29. Suzuki YJ and Packer L. Inhibition of NF-kappa B DNA binding activity by alpha-tocopheryl succinate. *Biochem Mol Biol Int* 31: 693–700, 1993.
30. Tetsuka T, Uranishi H, Sanda T, Asamitsu K, Yang JP, Wong–Staal F, and Okamoto T. RNA helicase A interacts with nuclear factor kappaB p65 and functions as a transcriptional coactivator. *Eur J Biochem* 271: 3741–3745, 2004.
31 Traenckner EB, Wilk S, and Baeuerle PA. A proteasome inhibitor prevents activation of NF-kappa B and stabilizes a newly phosphorylated form of I kappa B-alpha that is still bound to NF-kappa B. *EMBO J* 13: 5433–5441, 1994.
32. Valko M, Morris H, and Cronin MT. Metals, toxicity and oxidative stress. *Curr Med Chem* 12: 1161–1208, 2005.
33. Wisdom SJ, Wilson R, McKillop JH, and Walker JJ. Antioxidant systems in normal pregnancy and in pregnancy-induced hypertension. *Am J Obstet Gynecol* 165: 1701–1704, 1991.
34. Zhong H, Voll RE, and Ghosh S. Phosphorylation of NF-kappa B p65 by PKA stimulates transcriptional activity by promoting a novel bivalent interaction with the coactivator CBP/p300. *Mol Cell* 1: 661–671, 1998.

Address reprint requests to:
Giovanni Musci
Dipartimento di Scienze e Tecnologie Agro-alimentari
Ambientali e Microbiologiche
Università del Molise
via F. De Sanctis
86100 Campobasso Italy

E-mail: musci@unimol.it

Date of first submission to ARS Central, December 28, 2005; date of acceptance, April 9, 2006.

This article has been cited by:

1. Chih-Hung Guo, Pei-Chung Chen, Kuan-Pin Lin, Min-Yi Shih, Wang-Sheng Ko. 2011. Trace Metal Imbalance Associated with Oxidative Stress and Inflammatory Status in anti-Hepatitis C Virus Antibody Positive Subjects. *Environmental Toxicology and Pharmacology* . [CrossRef]
2. Helen J. MacGregor, Yoji Kato, Lindsay J. Marshall, Thomas G. Nevell, Janis K. Shute. 2011. A copper–hydrogen peroxide redox system induces dityrosine cross-links and chemokine oligomerisation. *Cytokine* . [CrossRef]
3. Catherine Gérard, Louis-Jean Bordeleau, Jake Barralet, Charles J. Doillon. 2010. The stimulation of angiogenesis and collagen deposition by copper. *Biomaterials* **31**:5, 824-831. [CrossRef]
4. Matthew K. McElwee, Min Ok Song, Jonathan H. Freedman. 2009. Copper Activation of NF-#B Signaling in HepG2 Cells. *Journal of Molecular Biology* **393**:5, 1013-1021. [CrossRef]
5. S. O. Simmons, C.-Y. Fan, R. Ramabhadran. 2009. Cellular Stress Response Pathway System as a Sentinel Ensemble in Toxicological Screening. *Toxicological Sciences* **111**:2, 202-225. [CrossRef]
6. Hesham M. Korashy, Ayman O. S. El-Kadi. 2008. NF-#B and AP-1 are key signaling pathways in the modulation of NAD(P)H:Quinone oxidoreductase 1 gene by mercury, lead, and copper. *Journal of Biochemical and Molecular Toxicology* **22**:4, 274-283. [CrossRef]
7. Hesham M. Korashy, Ayman O.S. El-Kadi. 2008. The role of redox-sensitive transcription factors NF-#B and AP-1 in the modulation of the Cyp1a1 gene by mercury, lead, and copper. *Free Radical Biology and Medicine* **44**:5, 795-806. [CrossRef]
8. Hao Tang, Yu Sun, Qingyu Xiu, Huiqi Lu, Huanxing Han. 2007. Cyclooxygenase-2 induction requires activation of nuclear factor of activated T-cells in Beas-2B cells after vanadium exposure and plays an anti-apoptotic role. *Archives of Biochemistry and Biophysics* **468**:1, 92-99. [CrossRef]